

## Two-terminal fault detection and location for hybrid transmission circuit

Muhd Hafizi Idris<sup>1</sup>, Mohd Rafi Adzman<sup>2</sup>, Hazlie Mokhlis<sup>3</sup>,

Mohammad Faridun Naim Tajuddin<sup>4</sup>, Haziha Hamid<sup>5</sup>, Melaty Amirruddin<sup>6</sup>

<sup>1,2,4,6</sup>Faculty of Electrical Engineering Technology, Universiti Malaysia Perlis, Arau, Malaysia

<sup>3</sup>Department of Electrical Engineering, Faculty of Engineering, Universiti Malaya, Kuala Lumpur, Malaysia

### Article Info

#### Article history:

Received Jan 19, 2021

Revised May 27, 2021

Accepted Jun 11, 2021

#### Keywords:

Fault detection

Fault location

Hybrid circuit

Impedance-based

Two-terminal

### ABSTRACT

This paper presents the algorithms developed to detect and locate the faults at a hybrid circuit. First, the fault detection algorithm was developed using the comparison of total positive-sequence fault current between pre-fault and fault times to detect the occurrence of a fault. Then, the voltage check method was used to decide whether the fault occurred at overhead line (OHL) or cable section. Finally, the fault location algorithm using the impedance-based method and negative-sequence measurements from both terminals of the circuit were used to estimate the fault point from local terminal. From the tests of various fault conditions including different fault types, fault resistance and fault locations, the proposed method successfully detected all fault cases at around 1 cycle from fault initiation and with correct faulted section identification. Besides that, the fault location algorithm also has very accurate results of fault estimation with average error less than 1 km and 1%.

*This is an open access article under the [CC BY-SA](https://creativecommons.org/licenses/by-sa/4.0/) license.*



### Corresponding Author:

Muhd Hafizi Idris

Faculty of Electrical Engineering Technology

Universiti Malaysia Perlis

Pauh Putra Campus, 02600 Arau, Malaysia

Email: hafiziidris@unimap.edu.my

## 1. INTRODUCTION

Fault is a phenomenon which can interrupt the supply of electricity to the customer. Most of the faults in power system occur at transmission or distribution lines because of their configuration which is exposed to the environment. After a fault has been detected by the protection relay [1], it must be located as soon as possible so that the repair works can be carried out and the line can be re-energized back into the network. The longer the outage time taken will make the power system be in stress condition for longer time because other lines must carry more loads and as the consequence this will reduce power system reliability and security. Fault location information is given by the intelligent electronic device (IED) such as numerical protection relay and disturbance recorder. These devices have internal fault location feature which will estimate the fault location once a fault has been detected. The accuracy of the given fault location information is depending on the algorithm, measurement inputs and parameters used inside this feature.

Fault location methods can be divided into different categories based on the measurement inputs used such as one-terminal [2]-[4], two-terminal [5]-[7] and wide-area methods [8]-[10]. One-terminal methods use the measurement inputs from one-end only thus it is the least accurate fault location methods. Furthermore, it uses many assumptions in fault location estimation due to many unknown parameters to locate the fault. However, this method is still widely used because there are still many standalone relays

installed in the substations across the network. Second are two-terminal methods which were introduced to eliminate the weakness of one-terminal methods by using measurements from both ends of the line. Thus, it has the highest accuracy among all fault location methods because many assumptions in fault location estimation can be avoided. The latest methods are wide-area fault location methods which use the strategically located measurements such as synchrophasor and phasor measurement unit (PMU). This method is still new to many utilities because it requires very high cost in installing the wide-area measurement systems (WAMS) [11].

Generally, there are two most widely used fault location methods which are impedance based [12]-[14] and travelling wave methods [15]-[17]. For impedance-based methods, there are many factors which can affect the fault location accuracy such as fault resistance [18], infeed and load currents [18], charging current [19], inaccurate fault type identification [20], uncertainty of zero-sequence impedance [21], non-homogeneity of the circuit [22], and many other factors. This paper focuses on the effects of circuit non-homogeneity on fault location accuracy. Based on work in [23], there are many conditions which can make a circuit in the network to be non-homogeneous such as different entrance and exit line structures, different designs of angle and tangent structures, different span and spacing sizes at different areas, combination of overhead line (OHL) and cable sections and many other factors. The circuit which uses the combination of OHL and cable is called as hybrid circuit. The fault location algorithms which assume that the circuit impedance parameters distributed uniformly along the circuit length can't be used to locate the fault at this hybrid circuit because both OHL and cable sections have different distributed parameters where for the same per unit length, OHL line has higher resistance compared to cable while on the other hand cable has higher capacitance compared to OHL.

There are several authors which focused on locating faults at non-homogeneous circuit. Liu *et al.* established the non-homogeneous model with fault by combining all generalized compact model of all homogeneous line sections [22]. Then, an additional state of the overall model was introduced to represent the fault location. Finally, the fault location was solved using the state estimation method. However, there is no explanation of how the fault was detected to occur before the method estimated the fault point. Travelling wave fault location for non-homogeneous line with multi-sections was proposed by Leite *et al.* by considering the effects of line parameters uncertainties [24]. Another travelling wave method was proposed by Hamidi and Livani for hybrid three-terminal circuits where the discrete wavelet transform (DWT) was used to extract the transient information from the measured voltages and to determine the arrival time of the wave [25]. However, travelling wave method is strongly dependent on the accuracy of detecting the wavefront. This wavefront might be weak to be detected typically in the case of high resistance fault. Moreover, travelling wave method also associated with complex solution because the method is performed using very high sampling frequency [26]. Artificial neural network (ANN) was used by Hatata *et al.* to classify and locate the fault at hybrid transmission circuit [27]. The weakness of this method is high number of training data is required to get the accurate results aside from the data must be trained for different fault types.

This paper proposes the fault detection and location algorithms for hybrid circuit. To detect the fault occurrence, total positive-sequence fault current is compared between pre-fault and fault times. Just after the total fault current more than the threshold value, a fault is detected. After that, to determine the correct faulted section, voltage check method is used by comparing the negative-sequence voltage for the point of connection between local and remote terminals. Finally, impedance-based method using the negative-sequence measurements from both terminals are used to estimate the fault location. One of the benefits of the proposed method is the fault type information is not required to detect and estimate the fault location. Besides that, the computation is much easier compared with the algorithms which solved for each phase because by using sequence values, only one computation needs to be solved for all types of fault.

## 2. PROPOSED FAULT DETECTION AND LOCATION ALGORITHMS FOR HYBRID CIRCUIT

This section presents the proposed fault detection and location algorithms using the measurements from both local and remote substations. Initially, the fault detection and location algorithms were derived to detect and locate the fault at a homogeneous circuit. Then, a modification on the algorithms was made to make the algorithms suitable to be used to detect and locate the faults at a hybrid non-homogeneous circuit.

The proposed fault detection algorithm uses the comparison of total fault current which flows toward the fault point between pre-fault and fault times to decide the occurrence of a fault. When a fault occurred at a line, local current,  $I_{L,F}$  and remote current,  $I_{R,F}$  will be flowing toward the fault point as shown in Figure 1. Hence, the total fault current,  $I_F$  will become very high compared to pre-fault value if both pre-fault local current,  $I_{L,PRE}$  and pre-fault remote current,  $I_{R,PRE}$  are added together as shown by (1).

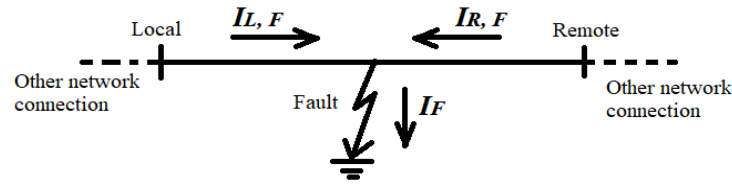


Figure 1. Local and remote currents flow during fault condition at a circuit

$$I_F \gg (I_{L,PRE} + I_{R,PRE}) \tag{1}$$

$$I_F = (I_{L,F} + I_{R,F}) \tag{2}$$

The algorithm proposed for fault detection only uses the positive-sequence values which can be converted directly from the phase values. This make the computation become easier compared with the computation which performed using the phase values. Both (1) and (2) then were converted into positive-sequence equations as shown by (3) and (4).

$$I_F^1 \gg (I_{L,PRE}^1 + I_{R,PRE}^1) \tag{3}$$

$$I_F^1 = (I_{L,F}^1 + I_{R,F}^1) \tag{4}$$

During normal condition, there will be no difference between  $I_F$  and the summation of  $I_{L,PRE}$  and  $I_{R,PRE}$  as shown by (5). The situation for normal condition is shown in Figure 2. At normal condition, the currents from both terminals will always be in the same direction where one will be exporting the power and the other one will be importing the power.

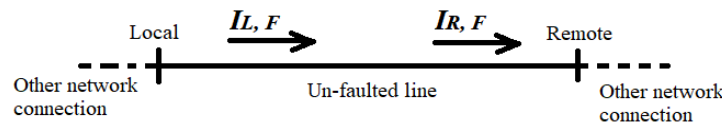


Figure 2. Local and remote currents flow during normal condition at a circuit

$$I_F^1 = (I_{L,PRE}^1 + I_{R,PRE}^1) \tag{5}$$

A threshold can be set to determine the fault occurrence as shown by (6).

$$I_F^1 > n \times (I_{L,PRE}^1 + I_{R,PRE}^1) \tag{6}$$

where,  $n > 1$  (constant)

The reason why the negative-sequence values are not chosen for the comparison of the total fault current between fault and pre-fault times is because during pre-fault, all phases are in balance condition, thus the negative-sequence values are very small and this will make it difficult to make the comparison.

Next is the fault location algorithm which was developed based on two-terminal fault location method. This method requires the measurements from both terminals. The measurements from both terminals are assumed to be synchronized. Figure 3 shows a transmission line with a fault at a point between local and remote terminals.

As can be seen from the Figure 3, a fault occurred at  $ml$  kilometre from local substation and  $(1-m)l$  kilometre from remote substation where  $m$  is the fault location in per unit and  $l$  is the line length in kilometre. The voltage at the fault point,  $V_F$  has equal values when measured from both ends. The currents from both terminals will flow through the fault point and through the fault resistance,  $R_F$  which is an unknown. The total of these two currents equal to the fault current,  $I_F$ . The voltage equations as seen from local and remote terminals are shown by (7) and (8) respectively.

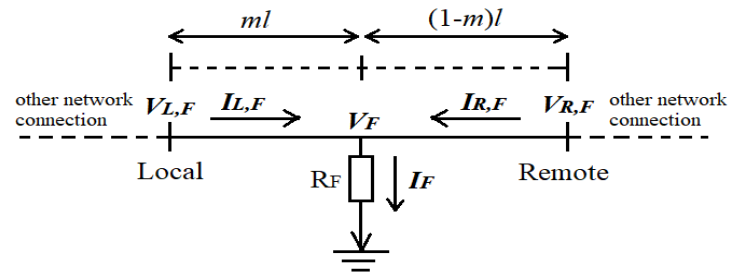


Figure 3. Transmission line with a fault between local and remote terminals

$$V_{L,F} = mlZ_{L-R}I_{L,F} + V_F \tag{7}$$

$$V_{R,F} = (1 - m)lZ_{L-R}I_{R,F} + V_F \tag{8}$$

where, the line impedance per km;

$$Z_{L-R} = R_{L-R} + jX_{L-R} \tag{9}$$

By arranging both (7) and (8) for  $V_F$ , we get (10) and (11).

$$V_F = V_{L,F} - mlZ_{L-R}I_{L,F} \tag{10}$$

$$V_F = V_{R,F} - (1 - m)lZ_{L-R}I_{R,F} \tag{11}$$

Then, both (10) and (11) were equalized as shown in (12) until (14).

$$V_{L,F} - mlZ_{L-R}I_{L,F} = V_{R,F} - (1 - m)lZ_{L-R}I_{R,F} \tag{12}$$

$$V_{L,F} - mlZ_{L-R}I_{L,F} = V_{R,F} - lZ_{L-R}I_{R,F} + mlZ_{L-R}I_{R,F} \tag{13}$$

$$V_{L,F} - V_{R,F} + lZ_{L-R}I_{R,F} = mlZ_{L-R}(I_{L,F} + I_{R,F}) \tag{14}$$

Next, (14) was arranged for  $m$  and we get;

$$m = \frac{V_{L,F} - V_{R,F} + lZ_{L-R}I_{R,F}}{lZ_{L-R}(I_{L,F} + I_{R,F})} \tag{15}$$

This research proposes the negative-sequence values as the inputs to fault location algorithm. Thus, the negative-sequence version for (15) is shown in (16). The result of this equation is in per unit and must be multiplied with the line length to get the estimated fault location in km. Line negative-sequence impedance,  $Z_{L-R}^2$  can be calculated based on (9) and using the positive-sequence parameters of the circuit.

$$m = \frac{V_L^2 - V_R^2 + lZ_{L-R}^2 I_R^2}{lZ_{L-R}^2 (I_L^2 + I_R^2)} \tag{16}$$

There are reasons why zero-sequence and positive-sequence values are not chosen as the inputs for the algorithm. The zero-sequence component only exists during ground faults thus not feasible to be used to estimate the fault location for ungrounded faults. For positive-sequence component, it exists in all types of fault including both symmetrical and un-symmetrical faults while the negative-sequence component only exists during un-symmetrical faults. However, the negative-sequence values are chosen instead of positive-sequence values because they are less affected by line charging current compared with the positive-sequence values.

The previous fault detection and location algorithms can be used to detect and locate the fault at homogeneous circuit which uses the same distributed circuit parameters along the circuit. However, for hybrid non-homogeneous circuit, a modification must be made because the circuit is consisting of OHL and cable sections where both sections have different distributed parameters. Figure 4 shows a hybrid circuit with X is the point of connection between OHL and cable sections.

To realize the previous fault detection and location algorithms to be used to detect and locate the fault at this type of circuit, both sections of the circuit must have separated fault detection algorithm. Once a fault has been detected to occur at any of those two sections, the fault location will be estimated by using the distributed parameters for that section. By using negative-sequence values, the voltage at the point of connection can be calculated based on the voltages from both terminals as shown by (17) and (18).

$$V_x^2 = V_R^2 - Z_{cable}^2 I_R^2 \tag{17}$$

$$V_x^2 = V_L^2 - Z_{OHL}^2 I_L^2 \tag{18}$$

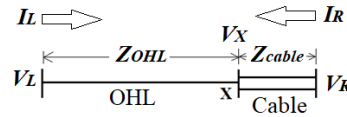


Figure 4. A hybrid circuit

In conjunction with using (6) to detect the occurrence of a fault at this circuit, the faulted section of this hybrid circuit can be determined using the voltage check method as follows;

- Fault at OHL section;

$$V_x^2 \text{ from (17)} < V_x^2 \text{ from (18)} \tag{19}$$

- Fault at cable section;

$$V_x^2 \text{ from (18)} < V_x^2 \text{ from (17)} \tag{20}$$

Once the actual faulted section has been determined, (16) will be used to estimate the fault location at the faulted section using the distributed parameters for that section. To measure the accuracy of the fault location estimation, (21) was used to compare the error between actual and estimated fault locations.

$$\% \text{ Error} = \frac{FL_{estimated} (km) - FL_{actual} (km)}{Line \text{ Length} (km)} \times 100 \tag{21}$$

### 3. MODELLING AND SIMULATION

This section presents the modelling and simulation of hybrid circuit and the fault detection and location algorithms. The hybrid circuit has been modelled using ATPDraw software and is displayed in Figure 5. The parameters for the circuit are given in Table 1. The distributed parameters for the OHL and cable sections were taken from the reference [28]. The rated voltage for the network is 220 kV and the nominal frequency is 50 Hz.

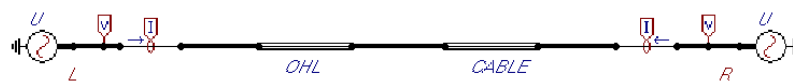


Figure 5. Hybrid circuit modelled using ATPDraw software

Table 1. Parameters for hybrid circuit [28]

Circuit Parameters	OHL	Cable
Length (km)	35	15
Positive-sequence Resistance, R <sub>1</sub>	0.038 Ω/km	0.024 Ω/km
Zero-sequence Resistance, R <sub>0</sub>	0.248 Ω/km	0.036 Ω/km
Positive-sequence Inductance, L <sub>1</sub>	0.896 mH/km	0.256 mH/km
Zero-sequence Inductance, L <sub>0</sub>	2.686 mH/km	0.332 mH/km
Positive-sequence Capacitance, C <sub>1</sub>	0.012997 μF/km	0.457627 μF/km
Zero-sequence Capacitance, C <sub>0</sub>	0.007124 μF/km	0.457627 μF/km

The measurements from local and remote terminals for each fault case were transferred to Matlab directory, loaded into Matlab workspace, and then were used by the fault detection and location algorithms. The OHL and cable subsystems which were developed using Matlab Simulink is presented in Figure 6. Inside both subsystems are the developed fault detection and location algorithms. The blocks inside OHL subsystem is shown in Figure 7. As can be seen from the figure, the measurements from both terminals are fed as the inputs to ‘POS SEQ’ and ‘NEG SEQ’ subsystems which are used to convert the phase values of the measurements to positive and negative-sequence values respectively. Then, the sequence values are used by the fault detection and location subsystems to detect the fault occurrence and locate the fault point for each section of the circuit. The blocks inside cable subsystem have the same form with the blocks in Figure 7.

As already mentioned earlier, to determine the actual faulted section between both sections, the voltage check method is used. Based on Figure 7, the fault detection subsystem has one more input from the voltage check subsystem which is used to determine whether the faulted section is OHL or cable section. The blocks inside this subsystem is exhibited in Figure 8. The blocks were arranged based on (19) for OHL section and (20) for cable section. The negative-sequence values are used as the inputs to this voltage check equations.

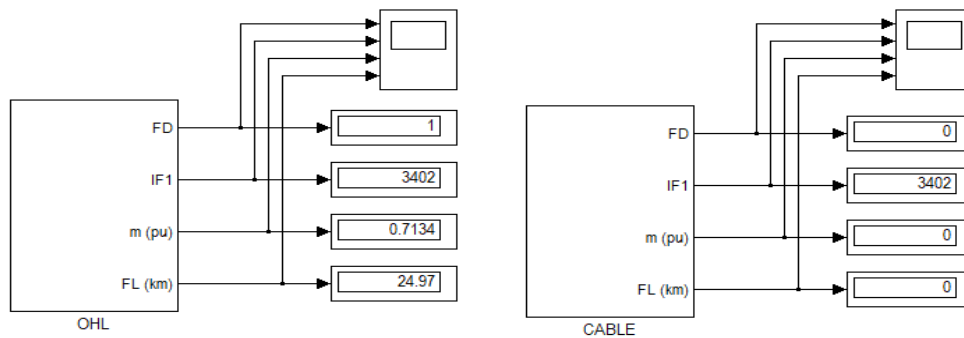


Figure 6. OHL and cable subsystems developed using Matlab Simulink

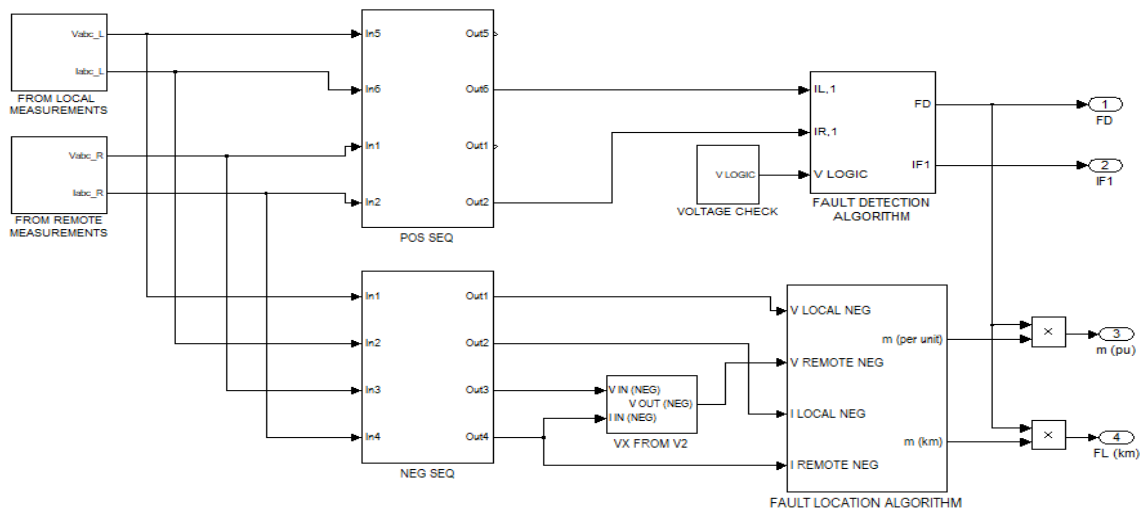


Figure 7. The blocks inside OHL subsystem

Next, the blocks inside fault detection algorithm are displayed in Figure 9 where the blocks were arranged based on (6). Both local and remote positive-sequence currents are added together to get the positive-sequence fault current,  $I_F$  and the value is measured and monitored for both fault and pre-fault conditions. The pre-fault value,  $I_{F,PRE}$  is continuously compared with the fault value,  $I_F$  and once the magnitude of  $I_F$  more than the threshold value, the fault is detected. The threshold value is equal with the threshold setting,  $n$  multiplied with the magnitude of the pre-fault value,  $I_{F,PRE}$ . The  $n$  was chosen to be 1.5 and the setting is sufficient because during fault condition, both local and remote currents will be in opposite direction making the total fault current becoming very high and the fault can be easily detected.

To realize the pre-fault value in the model, the transport delay (dashed box in Figure 9) block is used to delay the summation of magnitude between positive-sequence local and remote currents for one cycle. The exact faulted section will only be determined when the algorithm get the signal from ‘V LOGIC’ input (dashed circle in Figure 9) which coming from the voltage check subsystem. To get a stable fault location value, there are two delay blocks used inside fault detection subsystem where once the total delayed time (2 cycles) has been elapsed, the simulation will be stopped and the value of the final estimated fault location will be taken at the instant of the stop time.

Another subsystem is the fault location subsystem and the blocks inside this subsystem is shown in Figure 10. The arrangement of the blocks is based on (16). This subsystem uses the negative-sequence values as the inputs to estimate the fault point. The circuit impedance is computed inside ‘COMPUTES Z1’ subsystem which was arranged based on (9) and the parameters for this subsystem are based on each section whether OHL or cable section.

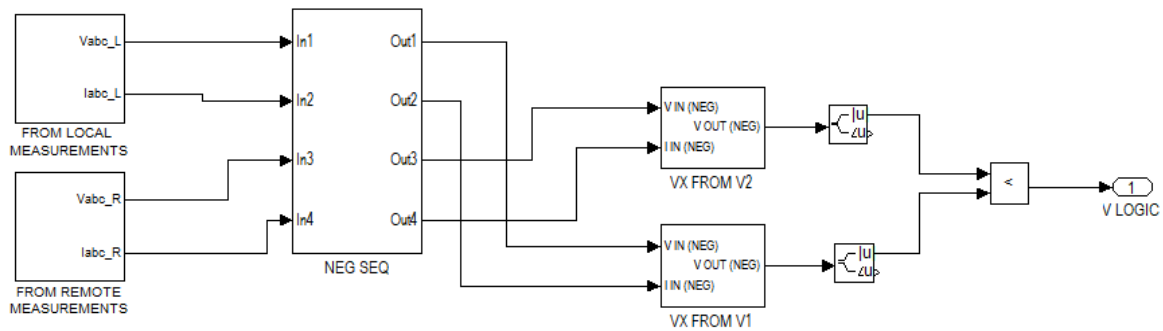


Figure 8. The blocks inside voltage check subsystem

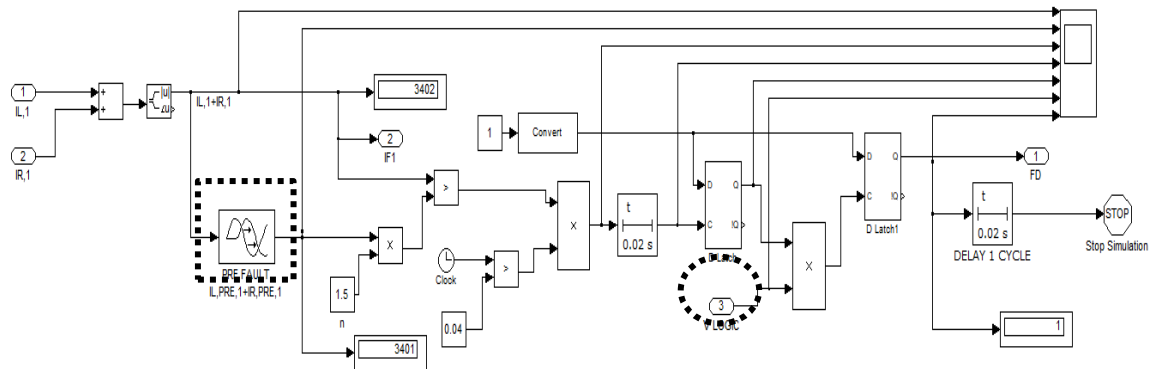


Figure 9. The blocks inside fault detection subsystem

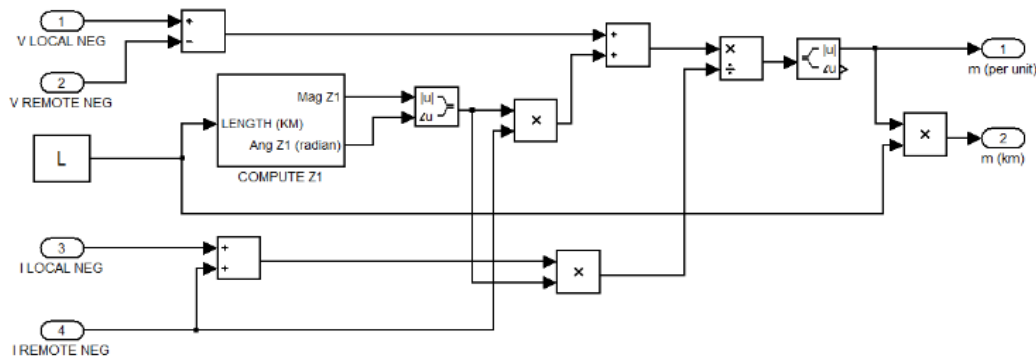


Figure 10. The blocks inside fault location subsystem

#### 4. SIMULATION RESULTS

This section presents the results of the proposed fault detection and location for the hybrid circuit. All estimated fault locations were measured from the local terminal for faults at both OHL and cable sections.

##### 4.1. Faults along the circuit with fixed fault type and fault resistance

The results of fault detection and location for faults along the circuit is presented in Table 2. The faults were fixed to single line-to-ground (SLG) fault type (phase A) with fault resistance,  $R_f=10 \Omega$ . All faults also had been initiated at 0.1 s and disappeared at 0.16 s. In the table, there are 6 faults at the OHL section, 1 fault at the point of connection between OHL and cable sections and 2 faults at the cable section.

In view of Table 2, it can be noticed that the proposed method successfully detected all faults along the hybrid circuit and correctly decided the faulted sections whether the faults occurred at OHL or cable sections. Both average and maximum errors for all faults are less than 1km and 1% which confirm the high accuracy of the developed fault location algorithm. For fault at the point of connection between OHL and cable sections (35km from local terminal), the two OHL and cable fault detectors identified the fault showing that the fault took place at a very near location or at the point of connection between OHL and cable sections and both detectors also give very accurate results of fault location for that fault case.

Table 2. Results of fault detection and location for faults along the circuit with fixed fault type and fault resistance

No	Actual Fault Section	Actual Fault Location (km)	Estimated Fault Location (km)	Detected Fault Section	Error (km)	Error (%)
1	OHL	5	5,014	OHL	0.014	0.028
2	OHL	10	10,020	OHL	0.020	0.040
3	OHL	15	15,010	OHL	0.010	0.020
4	OHL	20	20,000	OHL	0.000	0.000
5	OHL	25	25,030	OHL	0.030	0.060
6	OHL	30	30,120	OHL	0.120	0.240
7	POINT OF CONNECTION	35	34,950	OHL	0.050	0.100
		35	35,320	CABLE	0.320	0.640
8	CABLE	40	40,200	CABLE	0.200	0.400
9	CABLE	45	45,020	CABLE	0.020	0.040
				Average	0.078	0.157
				Maximum	0.320	0.640

##### 4.2. The effects of fault resistance on fault location accuracy

This test was performed to study the effects of fault resistance on the accuracy of the developed fault location. Fault resistance is an unknown value in fault location and the value is depending on the nature of the fault itself. In this study, double line-to-ground (LLG) fault (phase AB) was chosen as the fault type where the locations of the fault were varied along the hybrid circuit. For each fault location, there are three fault cases with different fault resistance values starting from low to high values which are 5, 50 and 100  $\Omega$ . All fault cases were initiated at 0.1 s. The results of errors for the fault location estimation are portrayed in Figure 11.

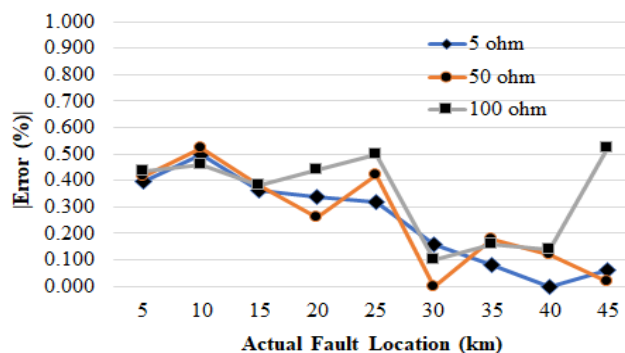


Figure 11. Fault location errors for different fault locations and fault resistance values

Based on the plot in Figure 11, it can be concluded as difficult to see the effects of fault resistance on the accuracy of the fault location estimation. The increase of fault resistance value does not add supplementary error to the fault location estimation. This is because the method uses the measurements from both terminals of the line thus the fault resistance parameter can be eliminated from the algorithm. This is not the case for the fault location algorithms which use the measurements from one-end only. The fault resistance parameter exists in those algorithms thus the variation of fault resistance value will influence the accuracy of fault location estimation.

**4.3. Different fault types and fault detection time**

The last test is for studying on the effects of different fault types on fault location estimation and for examining the fault detection time. The results of fault location error and fault detection time are given in Table 3 where all fault cases were initiated at 0.1 s. Based on the table, different fault types have been simulated which are single line-to-ground (SLG) fault, line-to-line (LL) fault, double line-to-ground (LLG) fault and three-phase (LLL) fault. For each fault type, fault location has been varied with three different fault locations for each OHL and cable section. Individual fault type also has been set to have different fault resistance value from other fault types. As been revealed earlier, the fault location algorithm uses the negative-sequence values as the inputs. Hence, theoretically, the algorithm not suitable to be used to locate the three-phase balanced fault where negative-sequence values do not exist. Nonetheless, in practical situation, there must be at least a slight difference of fault resistance values between different phases. In such a way, a small difference in fault resistance values will make the fault to be in imbalance condition and as the consequence, the negative-sequence values will exist. Notice that for three-phase (LLL) fault in Table 3, the fault resistance between phase A and B ( $R_{F(AB)}$ ) has been set to have a small difference with the fault resistance between phase B and C ( $R_{F(BC)}$ ).

As the summary from Table 3, all faults have been successfully detected and located. The average fault detection time is 0.1245 s which is 0.0245 s (1.225 cycle) measured from fault initiation time (0.1 s). In this way, this proved that the proposed fault detection can be used to quickly detect the fault occurrence at around 1 cycle for hybrid circuit and will accurately determine the faulted section.

The average and maximum errors for all fault cases which combined different fault conditions are less than 1 % and 1 km which show the high accuracy of the developed fault location algorithm. Lastly, the algorithm also proved that it can be used to detect and locate the three-phase (LLL) faults accurately with small imbalance of fault resistance between different phases.

Table 3. Results of fault detection time and fault location estimation for different fault types

No	Fault Types	Fault Resistance (ohm)	Actual Fault Section	Actual Fault Location (km)	Detected Fault Section	Estimated Fault Location (km)	Error (km)	Error (%)	Fault Detection Time (s)	Fault Detection Time-Fault Initiation Time (s)	
1	SLG	10	OHL	9	OHL	9,195	0.195	0.390	0.1265	0.0265	
2			OHL	18	OHL	18,200	0.200	0.400	0.1265	0.0265	
3			OHL	27	OHL	27,020	0.020	0.040	0.1265	0.0265	
4			CABLE	39	CABLE	39,190	0.190	0.380	0.1265	0.0265	
5			CABLE	43	CABLE	43,100	0.100	0.200	0.1265	0.0265	
6			CABLE	47	CABLE	47,040	0.040	0.080	0.1265	0.0265	
7	LL	30	OHL	9	OHL	9,209	0.209	0.418	0.1230	0.0230	
8			OHL	18	OHL	18,180	0.180	0.360	0.1235	0.0235	
9			OHL	27	OHL	27,120	0.120	0.240	0.1235	0.0235	
10			CABLE	39	CABLE	39,080	0.080	0.160	0.1235	0.0235	
11			CABLE	43	CABLE	43,040	0.040	0.080	0.1235	0.0235	
12			CABLE	47	CABLE	47,000	0.000	0.000	0.1235	0.0235	
13	LLG	50	OHL	9	OHL	9,283	0.283	0.566	0.1235	0.0235	
14			OHL	18	OHL	18,170	0.170	0.340	0.1240	0.0240	
15			OHL	27	OHL	27,150	0.150	0.300	0.1240	0.0240	
16			CABLE	39	CABLE	38,960	0.040	0.080	0.1235	0.0235	
17			CABLE	43	CABLE	42,940	0.060	0.120	0.1235	0.0235	
18			CABLE	47	CABLE	46,980	0.020	0.040	0.1235	0.0235	
19	LLL	$R_{F(AB)} = 68 \Omega, R_{F(BC)} = 72 \Omega$	OHL	9	OHL	9,202	0.202	0.404	0.1245	0.0245	
20			OHL	18	OHL	18,170	0.170	0.340	0.1245	0.0245	
21			OHL	27	OHL	27,150	0.150	0.300	0.1245	0.0245	
22			CABLE	39	CABLE	39,140	0.140	0.280	0.1245	0.0245	
23			CABLE	43	CABLE	43,040	0.040	0.080	0.1245	0.0245	
24			CABLE	47	CABLE	47,060	0.060	0.120	0.1245	0.0245	
							Average	0.119	0.238	0.1245	0.0245
							Maximum	0.283	0.566	0.1265	0.0265

## 5. CONCLUSION

This paper has successfully presented the proposed fault detection and location for hybrid circuit which has the combination of OHL and cable sections. First, the fault detection algorithm will detect the fault occurrence followed by determining the actual faulted section. Then, fault location algorithm will estimate the fault point from local terminal using the distributed parameters for the faulted section. By using the sequence values, the computation is easier compared with the algorithms which perform the computation using the phase values. Besides that, the method presented also does not need the fault type information and it shows the high accuracy of the fault detection and location for various fault conditions including the three-phase fault with small imbalance of fault resistance between different phases.

## ACKNOWLEDGEMENTS

The authors would like to acknowledge the support from the Fundamental Research Grant Scheme (FRGS) under a grant number of FRGS/1/2019/TK07/UNIMAP/03/2 from the Ministry of Higher Education Malaysia.

## REFERENCES

- [1] M. H. Idris, N. H. Hussin, M. B. Amiruddin, and S. Ahmad, "Modeling and Simulation of Inverse Time Overcurrent Relay Using Matlab/Simulink," in *IEEE International Conference on Automatic Control and Intelligent Systems (I2CACIS)*, 2016, pp. 40–44.
- [2] K. Ramar, H. S. Low, and E. E. Ngu, "One-end impedance based fault location in double-circuit transmission lines with different configurations," *Int. J. Electr. Power Energy Syst.*, vol. 64, pp. 1159–1165, Jan. 2015, doi: 10.1016/j.ijepes.2014.09.006.
- [3] O. Naidu, N. George, and Ashok S., "An accurate fault location method for radial distribution system using one terminal data," in *2015 International Conference on Technological Advancements in Power and Energy (TAP Energy)*, 2015, pp. 187–192, doi: 10.1109/TAPENERGY.2015.7229615.
- [4] A. Swetapadma and A. Yadav, "A novel single-ended fault location scheme for parallel transmission lines using k-nearest neighbor algorithm," *Comput. Electr. Eng.*, vol. 69, no. May, pp. 41–53, Jul. 2018, doi: 10.1016/j.compeleceng.2018.05.024.
- [5] F. V. Lopes *et al.*, "Practical Methodology for Two-Terminal Traveling Wave-Based Fault Location Eliminating the Need for Line Parameters and Time Synchronization," *IEEE Trans. Power Deliv.*, vol. 34, no. 6, pp. 2123–2134, Dec. 2019, doi: 10.1109/TPWRD.2019.2891538.
- [6] F. Poudineh-Ebrahimi and M. Ghazizadeh-Ahsaei, "Accurate and comprehensive fault location algorithm for two-terminal transmission lines," *IET Gener. Transm. Distrib.*, vol. 12, no. 19, pp. 4334–4340, Oct. 2018, doi: 10.1049/iet-gtd.2018.6084.
- [7] J. R. Gama, E. J. Leite, and F. V. Lopes, "Parametric analysis of two-terminal fault location methods based on unsynchronized data," in *2018 Simposio Brasileiro de Sistemas Eletricos (SBSE)*, 2018, pp. 1–6, doi: 10.1109/SBSE.2018.8395713.
- [8] M. H. Idris, M. Rafi Adzman, M. Faridun, N. Tajuddin, and A. Z. Abdullah, "Wide Area Fault Location for Power Transmission Network using Reactance Based Method," in *2018 IEEE 7th International Conference on Power and Energy (PECon)*, 2018, pp. 138–143, doi: 10.1109/PECON.2018.8684031.
- [9] S. H. Mortazavi, M. H. Javidi, and E. Kamyab, "Robust Wide Area Fault Location Considering Network Parameters Error," *IEEE Trans. Power Deliv.*, vol. 34, no. 3, pp. 786–794, Jun. 2019, doi: 10.1109/TPWRD.2019.2897402.
- [10] Z. Li, Y. Cheng, X. Wang, Z. Li, and H. Weng, "Study on wide-area traveling wave fault line selection and fault location algorithm," *Int. Trans. Electr. Energy Syst.*, vol. 28, no. 12, Dec. 2018, doi: 10.1002/etep.2632.
- [11] R. B. Sharma and G. M. Dhole, "Wide Area Measurement Technology in Power Systems," *Procedia Technol.*, vol. 25, no. Raerest, pp. 718–725, 2016, doi: 10.1016/j.protcy.2016.08.165.
- [12] M. Nemati, M. Bigdeli, and A. Ghorbani, "Impedance-Based Fault Location Algorithm for Double-Circuit Transmission Lines Using Single-End Data," *J. Control. Autom. Electr. Syst.*, vol. 31, no. 5, pp. 1267–1277, Oct. 2020, doi: 10.1007/s40313-020-00620-w.
- [13] L. Wang, Z. Deng, and M. Ma, "Fault Location Method for Distribution Network Based on Improved Apparent Impedance," in *2019 IEEE Sustainable Power and Energy Conference (iSPEC)*, 2019, pp. 2556–2560, doi: 10.1109/iSPEC48194.2019.8974882.
- [14] S. Didehvar and R. Mohammadi Chabanloo, "Accurate estimating remote end equivalent impedance for adaptive one-ended fault location," *Electr. Power Syst. Res.*, vol. 170, no. December 2018, pp. 194–204, May 2019, doi: 10.1016/j.epsr.2019.01.011.
- [15] M. Parsi, P. Crossley, P. L. Dragotti, and D. Cole, "Wavelet based fault location on power transmission lines using real-world travelling wave data," *Electr. Power Syst. Res.*, vol. 186, no. June, p. 106261, Sep. 2020, doi: 10.1016/j.epsr.2020.106261.
- [16] Z. Jianwen, H. Hui, G. Yu, H. Yongping, G. Shuping, and L. Jianan, "Single-phase ground fault location method for distribution network based on traveling wave time-frequency characteristics," *Electr. Power Syst. Res.*, vol. 186, no. March, p. 106401, Sep. 2020, doi: 10.1016/j.epsr.2020.106401.

- [17] Y. Shi, T. Zheng, and C. Yang, "Reflected Traveling Wave Based Single-Ended Fault Location in Distribution Networks," *Energies*, vol. 13, no. 15, p. 3917, Jul. 2020, doi: 10.3390/en13153917.
- [18] M. H. B. Idris, "Combination effects of fault resistance and remote in feed current on simple impedance based fault location," *Conference: 2nd International Conference on Emerging Electrical Energy, Electronics and Computing Technologies 2020 (ICE4CT 2020)*, Jan. 2020, doi: 10.1088/1742-6596/1432/1/012002.
- [19] Y. Xue, D. Finney, and B. Le, "Charging Current in Long Lines and High-Voltage Cables – Protection Application Considerations," in *67th Annual Georgia Tech Protective Relaying Conference*, 2013.
- [20] G. M. Gadge and S. S. Hadpe, "Techniques for Location of Fault on Transmission Lines in Power System," *Int. Res. J. Eng. Technol.*, vol. 5, no. 7, pp. 903–908, 2018, doi: 10.5539/mas.v4n8p63.
- [21] S. Das, S. N. Ananthan, and S. Santoso, "Estimating Zero-Sequence Line Impedance and Fault Resistance Using Relay Data," *IEEE Trans. Smart Grid*, vol. 10, no. 2, pp. 1637–1645, Mar. 2019, doi: 10.1109/TSG.2017.2774179.
- [22] Y. Liu, B. Wang, X. Zheng, D. Lu, M. Fu, and N. Tai, "Fault Location Algorithm for Non-Homogeneous Transmission Lines Considering Line Asymmetry," *IEEE Trans. Power Deliv.*, vol. 35, no. 5, pp. 2425–2437, Oct. 2020, doi: 10.1109/TPWRD.2020.2968191.
- [23] P. S. R. Committee, "AC Transmission Line Model Parameter Validation," *IEEE Power & Energy Society*, 2014.
- [24] E. J. S. Leite, F. V. Lopes, F. B. Costa, and W. L. A. Neves, "Closed-Form Solution for Traveling Wave-Based Fault Location on Non-Homogeneous Lines," *IEEE Trans. Power Deliv.*, vol. 34, no. 3, pp. 1138–1150, Jun. 2019, doi: 10.1109/TPWRD.2019.2900674.
- [25] R. J. Hamidi and H. Livani, "A travelling wave-based fault location method for hybrid three-terminal circuits," in *2015 IEEE Power & Energy Society General Meeting*, vol. 2015, 2015, doi: 10.1109/PESGM.2015.7286247.
- [26] E. Personal, A. García, A. Parejo, D. Larios, F. Biscarri, and C. León, "A Comparison of Impedance-Based Fault Location Methods for Power Underground Distribution Systems," *Energies*, vol. 9, no. 12, p. 1022, Dec. 2016.
- [27] A. Y. Hatata, Z. M. Hassan, and S. S. Eskander, "Transmission Line Protection Scheme for Fault Detection , Classification and Location Using ANN," *International Journal of Modern Engineering Research*, vol. 6, no. August, pp. 1–10, 2016.
- [28] T.-C. Lin, P.-Y. Lin, and C.-W. Liu, "An Algorithm for Locating Faults in Three-Terminal Multisection Nonhomogeneous Transmission Lines Using Synchrophasor Measurements," *IEEE Trans. Smart Grid*, vol. 5, no. 1, pp. 38–50, Jan. 2014, doi: 10.1109/TSG.2013.2286292.